

Reinforcement of mechanical properties in unsaturated polyester resin with nanosheet

Vahid Zarei*^{1,2}

¹Department of Petroleum and Chemical Engineering, Science and Research Branch, Islamic Azad University (IAU), Tehran 1477893855, Iran

²Department of Materials Science and Engineering, School of Engineering, Shiraz University, Zand Ave, Shiraz, Iran

(Received April 13, 2021, Revised November 22, 2023, Accepted November 23, 2023)

Abstract. In the oil and gas industry, composite materials should exhibit high flexibility and strength for offshore structures. Therefore, weak points in the composites should be improved, such as brittleness, moisture penetration, and diffusion of detrimental ions into nanometric pores. This study aimed to increase the strength, flexibility, and plugging of nanopores using single-layer graphene oxide (SGO) nanosheets. Therefore, SGO is added to unsaturated polyester resin at concentrations of 0.015 and 0.15 % with Normal Methyl Pyrrolidone (NMP) as a solvent for the formation of Nanographene Oxide Reinforced Polymer (NGORP). The mechanical properties of the prepared samples were tested using tensile testing (ASTM-D 638). It has been shown that incorporating SGO, approximately 0.015%, into the base resin resulted in enhanced properties such as rupture resistance forces increased by 745.61 N, applied stress tolerances increased by 4.1 MPa, longitude increased to 1.58 mm, elongation increased by about 2.38%, and rupture energy increased by about 204.51 J. Despite the decrease in tensile force strength properties in the manufactured nanocomposite with 0.15% SGO, it has exclusive flexibility properties such as a high required energy level for rupture of 5,576 times and a formability of 40% more than the base sample. It would be best to use NGORP manufactured from 0.015% nanosheets with exclusive properties rather than base samples for constructing parts and equipment, such as rebars, composite sheets, and transmission pipes, on offshore platforms.

Keywords: flexibility; graphene oxide nanosheets; mechanical strength; nanocomposite; offshore platform

1. Introduction

Several studies have shown that nanostructures are compounds with dimensions between 1 and 100 nm (Zarei and Nasiri 2021, Zarei *et al.* 2021). The materials generally have three dimensions: length, width, and height. Materials are classified as nanostructured if at least one of these dimensions is in the nanometer scale (Feng *et al.* 2023, Mirzaasadi *et al.* 2021).

Nanostructured materials can be classified into different categories based on their nanotechnology. Free dimensions are one such division. A free dimension refers to a dimension that is not at the nanoscale and can have any value. Accordingly, nanomaterials can be categorized as nanoparticles, nanowires, thin films, and bulk nanomaterials.

Zero-dimensional nanomaterials refer to materials whose dimensions are all less than 100 nm, meaning that no dimension exceeds 100 nm, such as nanoclusters. Materials with one dimension greater than 100 nm will be placed in the category of one-dimensional (1D) nanomaterials, for example, CNT (See Fig. 1).

Materials with two-dimensions greater than 100 nm are classified as two-dimensional (2D) nanomaterials, including nanosheets, nanolayers, and graphene oxides. Materials

with three dimensions larger than 100 nm are classified as three-dimensional (3D) nanomaterials. This group of materials consists of materials with pores in the nanometer range (Micro or Mesoporous Nanomaterials) or particles dispersed within the matrix with at least one dimension in the nanometer range (Graphene oxide nanocomposites).

Solid materials with pores can be categorized into three types based on pore size. Solid materials with a pore size of 2 nm or less than 2 nm are included in materials containing micropores. Materials with pore sizes ranging from 2 to 50 nm were classified as mesopores, and those with pore sizes larger than 50 nm were classified as macropores (Davis 2002, Zarei *et al.* 2023).

When particles are nanoscale, their physical and chemical properties can be significantly altered compared to those of micron-sized particles. Generally, when powder reinforcement is added to polymers, there are few interactions between the reinforcement and the polymer. In contrast, the interactions are more significant if the reinforcement particles are smaller. If these particles reach the sizes of atoms or molecules, their strengthening properties are maximized. When materials are synthesized at the nanometer scale, new features can be added, which cannot be observed in larger dimensions (Pokropivny and Skorokhod 2007).

Researchers have sought to improve the mechanical and chemical properties of materials to prevent corrosion because corrosion factors decrease the properties and life of a material. Recently, some researchers have reported the

*Corresponding author, Mr.,
E-mail: vahid.zarei@srbiau.ac.ir

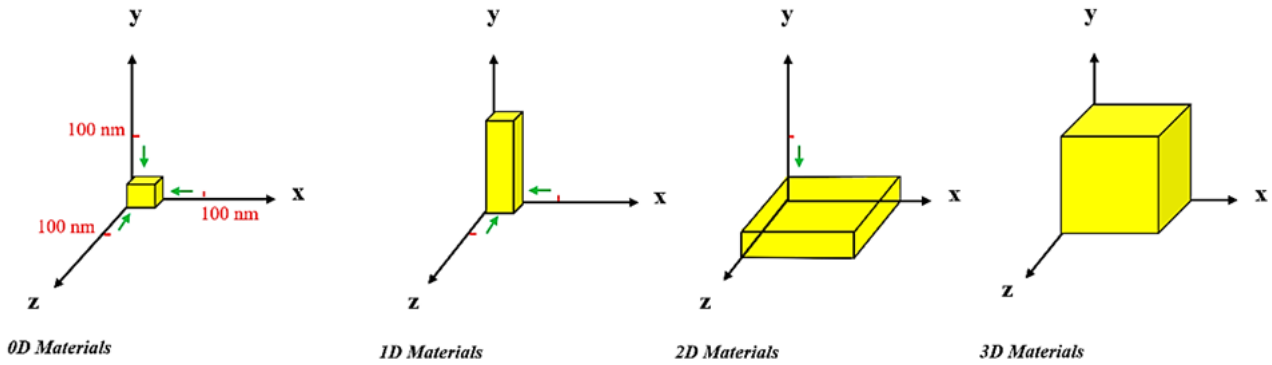


Fig. 1 Categorization of Nanomaterials according to free dimensions

corrosion resistance of nanostructured materials (nanocomposites), which shows that nanoscale materials have unique physical and chemical properties that increase corrosion resistance (Chandradass *et al.* 2008).

On Offshore and Onshore drilling rigs, composite materials should be highly resistant to seawater pH, salts, corrosive materials, water penetration, and algae growth. Additionally, their resistance to UV rays, air moisture, and physical factors such as wave impact should be considered in their designation. In comparison to traditional materials, such as steel, metal, and alloys, fiber-reinforced polymers (FRP) have excellent stiffness and corrosion resistance (Hammami and Al-Ghuilani 2004, Signor *et al.* 2003).

FRPs have a high strength-to-weight ratio and are highly corrosion-resistant, which makes them an effective alternative to steel (Park *et al.* 2007). Corrosion-resistant FRP can be used as reinforcing materials for different structures to increase their life expectancies (Bouguerra *et al.* 2011). It is important to remember that when flexibility is required, FRP will be limited, and steel will be the best choice (Won *et al.* 2008, 2007). Despite the various excellent functions and potential applications of FRPs, fibers and their matrices can be damaged or destroyed under improper conditions in sea environments.

According to previous studies, carbon nanomaterials can enhance composite properties and eliminate their flaws (Khayat *et al.* 2021, Farazin and Mohammadimehr 2020, Javani *et al.* 2019). Shokrieh *et al.* (2013) showed that 0.15% of multi-walled carbon nanotubes MWCNT added to UP composites increased the tensile and bending strength by 6 and 20%, respectively (Shokrieh *et al.* 2013).

It has been demonstrated that adding CNTs to resins can improve some properties (Bousahla *et al.* 2020, Medani *et al.* 2019, Tounsi *et al.* 2013) but can also cause problems during the application process. One of these problems is that nanotubes, with their long and narrow structures, aggregate with each other to form intertwined aggregates. As a result, the viscosity increases improperly, whereas the nanosheets can slip over each other freely and prevent excessive viscosity. Accordingly, nanosheets, which are less expensive than nanotubes, were utilized in this study to solve problems and enhance the properties of the UPR resin (Jang and Zhamu, 2008).

In the realm of polymers, unsaturated polyester resin (UPR) is renowned as a thermosetting polymer for its

affordability and resistance to temperature. These attributes have rendered it a fitting material across diverse industries, finding applications in coatings, structural constructions, transportation, storage tanks, and transmission pipes. Unlike epoxy resins, these thermosetting polymers are prone to shrinkage during curing and exhibit comparatively lower tensile and stiffness strengths. Addressing these limitations, integrating nanomaterials into polymer matrices offers a promising avenue to enhance the stiffness and tensile strength of UPR resins and curb shrinkage. This study aimed to augment the mechanical properties of UPR by integrating graphene oxide nanosheets and addressing the issue of shrinkage (Huang *et al.* 2020).

2. Materials and methods

2.1 Materials

Single-layer graphene oxide (SGO) with a high specific surface area (SSA) and a purity of 99.9% was purchased from the United Nanotech Innovation Company. SGO was selected because of its unique properties that distinguish it from other carbon nanomaterials. Dispersibility in solvents and polymers is one feature of this material. The higher dispersion of graphene oxide nanosheets in polymer resins prevents their aggregation, so weak points in the matrix are not created. SGO nanomaterials have a single-layer structure and a high surface area, which results in more significant chemical activity. The increase in chemical activity strengthens the chemical bonds between the polymer molecules and the matrix, enhancing the mechanical strength of the polymer. Dispersing SGO is done with N-Methyl-2-pyrrolidone, commonly called NMP, which is 99.9% pure and manufactured by Merck. Other materials in this project have laboratory chemical grades and were used without impurities.

2.2 Methods

2.2.1 Constructing silicon mold

Dog-bone specimens were constructed using an aluminum alloy following ASTM-D 638 (TAPE-I). After filling the mold with silicone resin, the samples were removed after 24 hr. An image of the manufactured mold is shown in Fig. 2.



Fig. 2 Construction of mold using dog-bone specimens



Fig. 3 UPR: before and after the dispersion of SGO



Fig. 4 Molding of pure UPR and NGORP

2.2.2 Dispersion of SGO in the base resin

In the first step, SGO was placed in NMP solvent using an ultrasonic machine, carried out in two steps for five min. Next, two samples of 0.15% and 0.015% of the previously prepared suspension were added to 100 cc of UPR so that the final nanocomposite contained 0.00015 and 0.0015 g of SGO, respectively. Subsequently, ultrasonic waves were used to disperse SGO in the resin for five min.

Fig. 3 shows a resin sample with SGO after ultrasonication. This picture shows that SGOs are dispersed uniformly and stably. Afterward, the samples containing SGO were placed in an oven for 24 hr at 60 °C under a dynamic vacuum to remove the solvent.

2.2.3 Fabrication of base sample and nanocomposite

A methyl ethyl ketone peroxide (MEKP) initiator with a weight concentration of 2% and a cobalt naphthalate accelerator with a weight concentration of 1% were added to the base resin, and resins containing SGO (outted from a vacuum oven). These samples were then poured into a silicone mold to prepare dog-bone samples of the base resin (purple) and the NGORP (black) (See Fig. 4). After 24 hr, the samples were outted from the molds and placed in an oven at 100 °C for 24 hr for post-curing.

3. Results and discussions

3.1 Results

3.1.1 Mechanical properties of fabricated samples

Tensile tests were performed on the samples according to the ASTM-D 638 standard to evaluate the mechanical properties of the prepared composites.

Base sample

A sample without SGO was prepared as a base sample to compare the effect of the nanosheets on the mechanical properties. A tensile test was performed on the base sample according to the ASTM-D 638 standard test. The results are shown in Fig. 5.

NGORP contains 0.015% SGO

The tensile result test for the NGORP sample with a concentration of 0.015% w/v SGO is shown in Fig. 6, and its mechanical properties are reported in Table 1.

As illustrated in Table 1, by adding SGO, the rupture tolerance force enhances 745.61 N; this increase in tolerance force is due to more chemical bonds created between Graphene Nanosheets and the polymeric matrix. The tolerance of applied stress in manufactured Nanocomposites was raised to 4.1 MPa. This increase results from the force distribution in existing Graphene sheets in the polymer matrix, perturbing the cracks and dissipating their energies. Another parameter promoted by the addition of SGO is flexibility because the length of the sample increased by 1.58 mm during the tensile test compared to the base sample. The increase in the sample's elongation containing SGO up to 2.38% compared to the base sample confirms the increasing flexibility properties.

After adding only 0.015% w/v percentages of SGO, one of the remarkable results is the significant increase of 2040 J in the sample's rupture's required energy. This increase in energy is due to the existence of Graphene sheets in the polymer matrix at the rupture point. Because the point of the nanocomposite where the rupture takes place requires spending more energy to overcome the friction caused by the separation of Graphene sheets from the polymer matrix, this issue increases the duration of time for tensile force tolerance by 14 sec more than the base sample.

NGORP contains 0.15% SGO

The ASTM-D 638 test results for NGORP samples containing 0.15% SGO (w/v) are depicted in Fig. 7. This sample's properties are compared with the base sample and detailed in Table 2.

Adding 0.15% SGO (w/v) decreased 1295.74 N in the

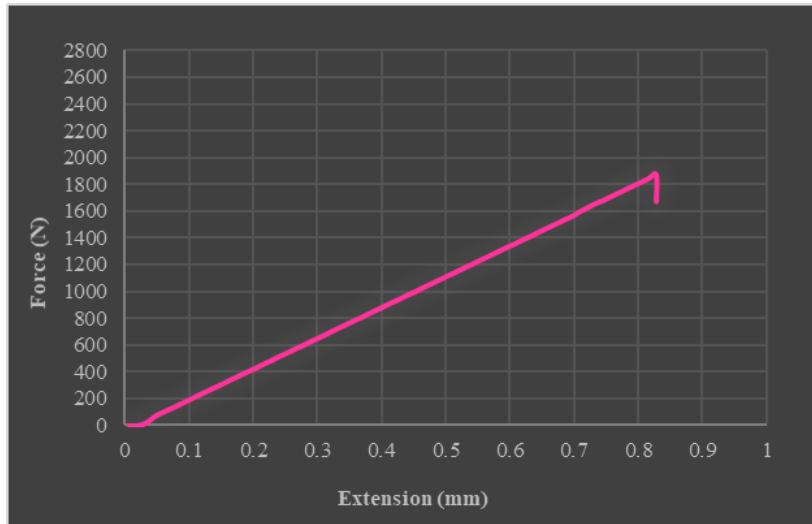


Fig. 5 ASTM-D638 test results on a base sample

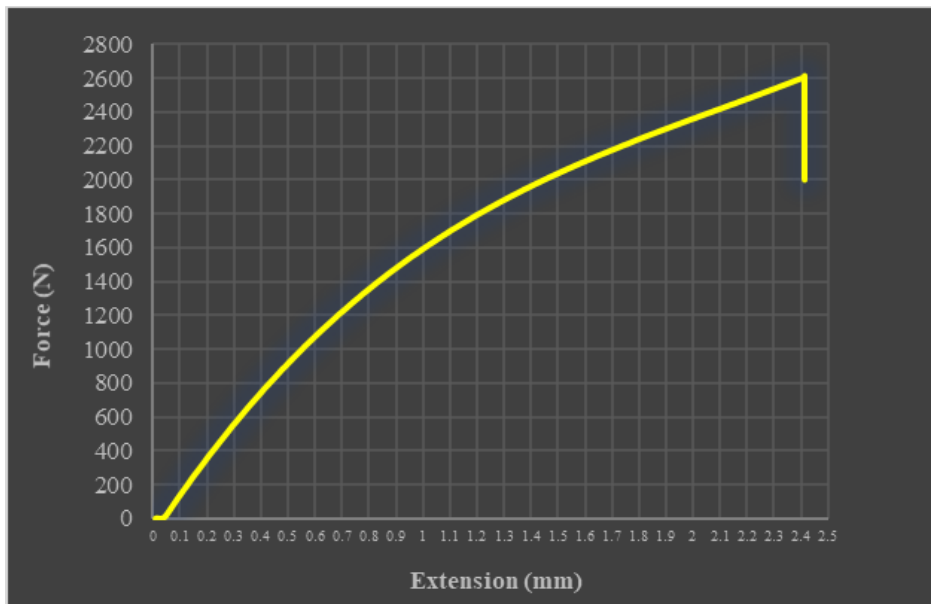


Fig. 6 ASTM-D638 test results of an NGORP composite incorporating 0.015% SGO

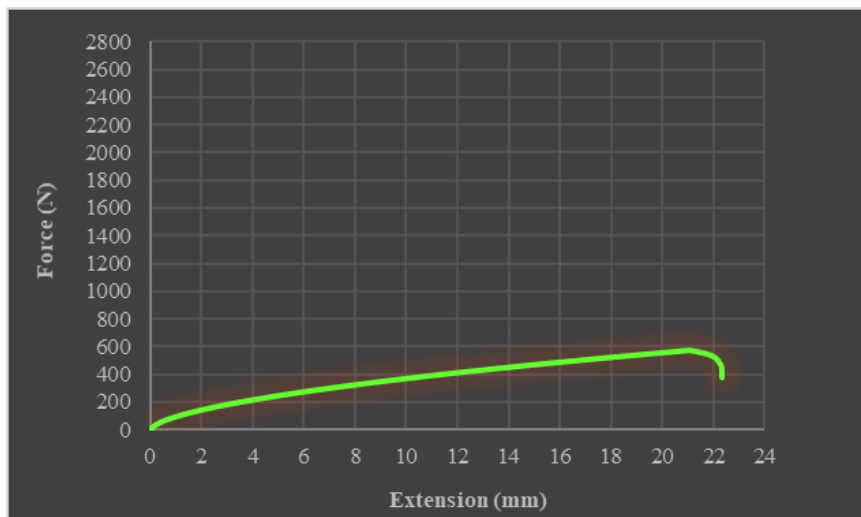


Fig. 7 ASTM-D638 test results on an NGORP composite containing 0.15% SGO

Table 1 Parameters obtained from the tensile test on NGORP- 0.015% SGO and base sample

Mechanical properties	Base	0.015% SGO	Change properties
Force (N)	1869.74	2615.35	+ 745.61
Extension (mm)	0.8287	2.4153	+ 1.5866
Stress (MPa)	12.4793	16.5979	+ 4.1186
Elongation (%)	1.6331	4.017	+ 2.3839
Energy (J)	690.5156	2731.033	+ 2040.5174
TIME (Min)	0:10:06	0:24:32	+ 0:14:26

Table 2 Parameters obtained from the tensile test on NGORP- 0.15% SGO and base sample

Mechanical properties	Base	0.15% SGO	Change properties
Force (N)	1869.74	574	-1295.74
Extension (mm)	0.8287	22.3223	+ 21.4936
Stress (MPa)	12.4793	3.8300	- 8.6493
Elongation (%)	1.6331	41.9244	+ 40.2913
Energy (J)	690.5156	6267.1316	+5576.616
TIME (Min)	0:10:06	4:15:59	+ 4:05:53



Fig. 8 The flexibility of NGORP-0.15% SGO



Fig. 9 Shrinkage of the base sample relative to nano-composites

rupture tolerance force compared to the base sample. Additionally, the sample's tolerance stress decreased by approximately 8.6 MPa. This reduction can be attributed to SGO aggregation caused by its increased concentration. Areas with aggregated SGO experience heightened stress concentration, ultimately contributing to the sample's failure.

One of the advantages of manufacturing this sample is its high flexibility (See Fig. 8). During the tensile test, the

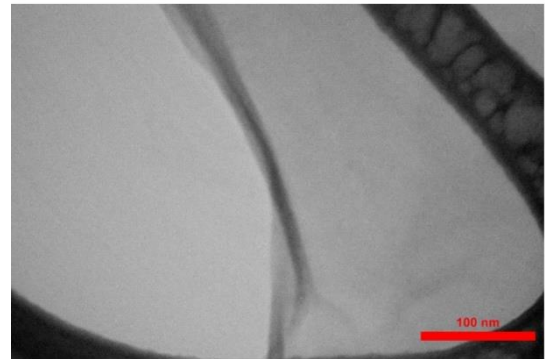
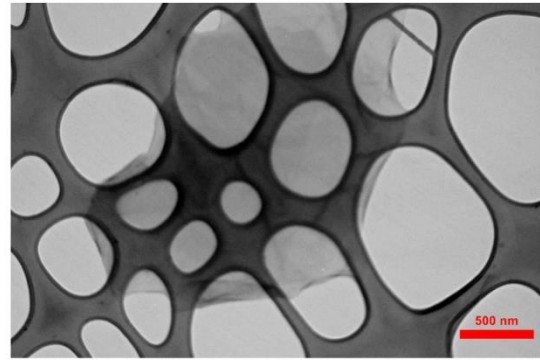


Fig. 10 TEM of SGO



Fig. 11 Image of GO with different functional groups and SGO in various solvents (After one day)



Fig. 12 Image of GO and SGO with different functional groups and SGO in various solvents (After 60 days)

sample's elongation and extension increased to 40.29% and 21.49 mm, respectively, compared to the base resin. This improved flexibility resulted in a 5576 J increase in the energy required for sample rupture compared to the base. Notably, in NGORP containing 0.15% SGO, the time for sample tolerance to rupture was extended to 4 min, a substantial difference from the base sample's 10 sec.

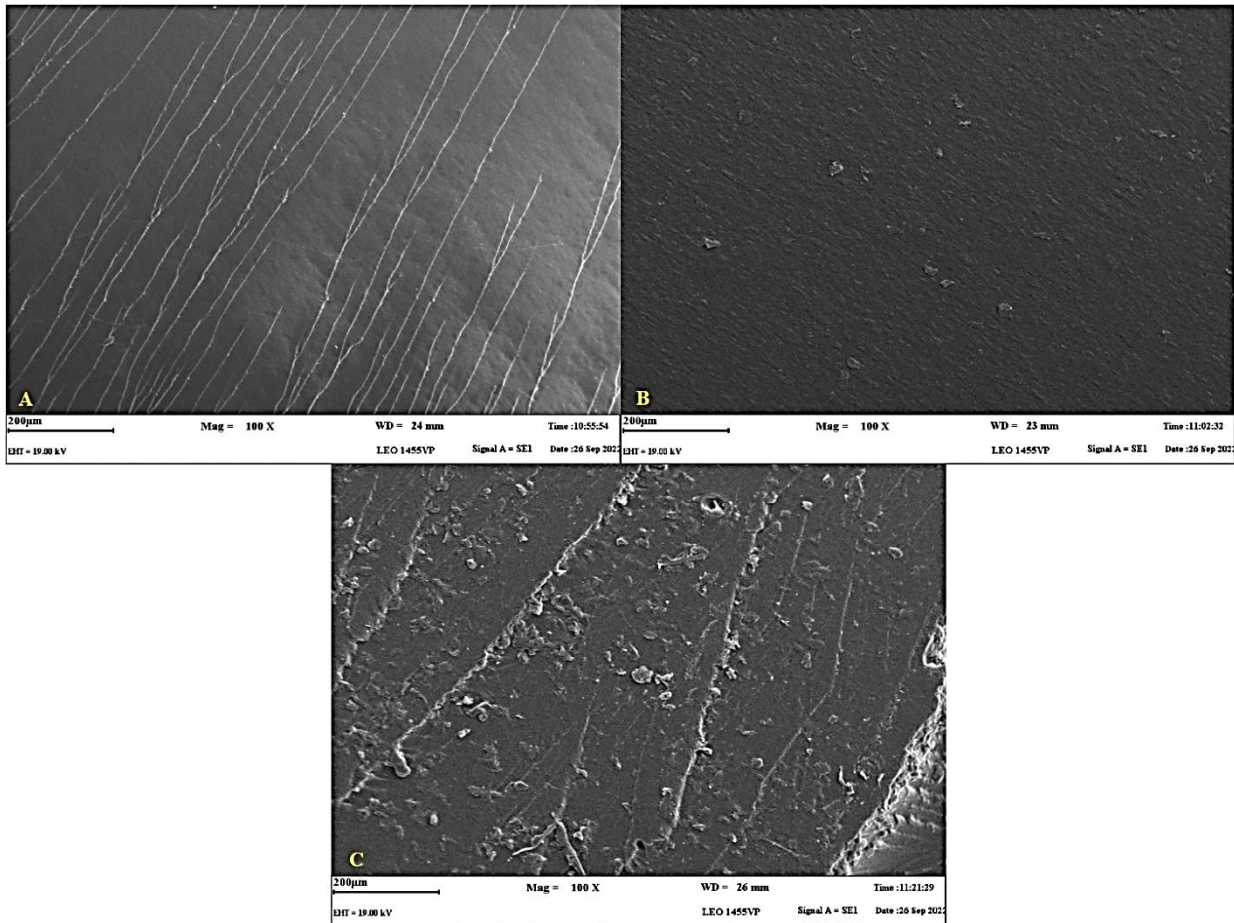


Fig. 13 SEM images from fracture surface area A) pure UPR, B) NGORP-0.015%, C) NGORP-0.15%

Shrinkage phenomenon

The shrinkage in UPR presents a significant drawback for this polymer, leading to various issues in constructing parts. As depicted in Fig. 9, shrinkage is evident in the base sample when using identical mold sizes, whereas this phenomenon is notably absent in nanocomposite samples.

3.2 Discussions

Characterization of SGO

The transmission electron microscope (TEM) apparatus model Zeiss LEO 906-Germany and Holey Carbon grids were applied to show the thickness and width of the SGO used. The results are reported in Fig. 10.

As seen in Fig. 10, the width and length of the Graphene sheets are more than 100 nm, while the thickness is less than 100 nm, which determines SGO in the category of two-dimensional Nanomaterials.

Stability of SGO

An experiment has been arranged to show the stability of single-layer Graphene oxide (SGO) in solvents compared to another Graphene oxide (GO). In this way, three GO were selected: one is a multilayer Graphene oxide with Hydroxyl functional group (GO-OH), the second is a multilayer Graphene oxide with Amine functional group (GO-NH₂), and the third is SGO. Two solvents, Methyl Ethyl ketone (MEK) and N-methyl-2-pyrrolidone (NMP)

were selected in the experiment design for the GO and SGO dispersion process. First, 1 gr of each, GO-OH, GO-NH₂, and SGO, were mixed in 30 cc of solvents. Then, in three-time intervals of 5 min, the ultrasonic process was carried out by the apparatus model BANDELIN made in Germany under a power of 150 W and energy of 120.093 KJ. After ultrasonication, all GO and SGO were poured into containers with a similar volume and kept at ambient temperature to investigate their stability versus time (See Fig. 11). The solutions were placed at a calm ambient for 60 days to evaluate their sedimentation rate and determine all GO's and SGO stability (See Fig. 12).

Fig. 11 illustrates the complete dispersion of SGO within (NMP) and (MEK) solvents. This dispersion mechanism is attributed to a confined layer of solvent near the SGO surface, preventing the aggregation of SGO sheets through steric hindrance. Typically, the dispersion of SGO in solvents involves sonication, generating shear stresses and cavitation in the solvent, allowing them to remain suspended for up to 60 days without sedimentation. Sustaining this dispersion necessitates the introduction of an energy barrier against aggregation. This barrier can be achieved through electrostatic or steric repulsion. The Brownian motion will maintain the dispersion when this energy barrier is sufficiently high (Johnson *et al.* 2015).

Microstructure of NGORP

The microstructure of pure resin and NGORPs were investigated with a scanning electron microscope (SEM)

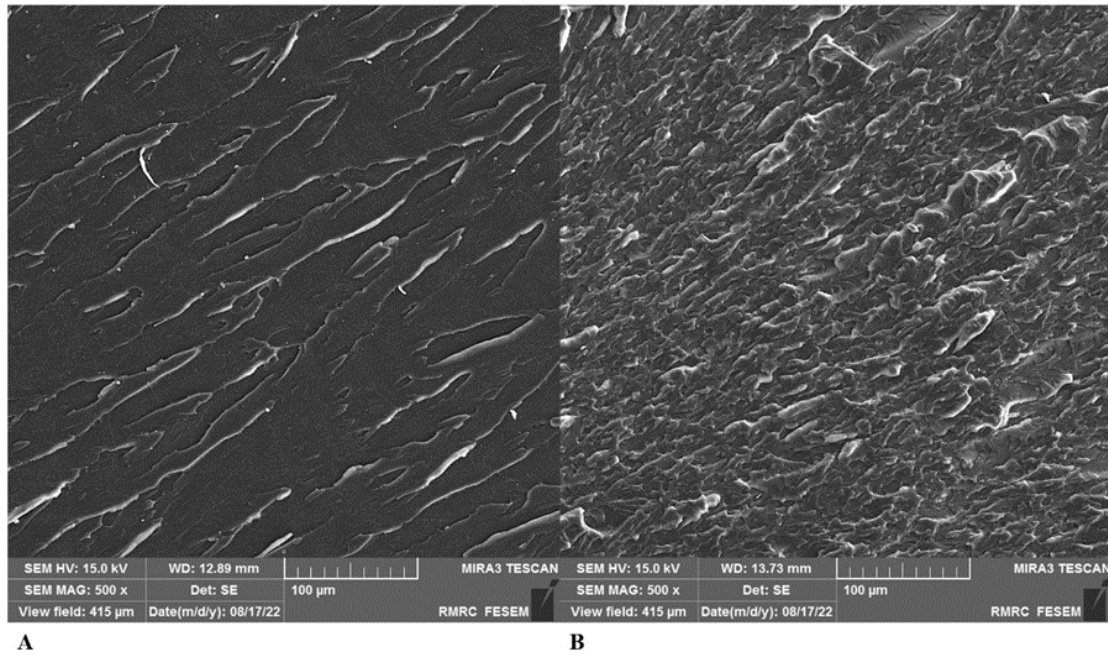


Fig. 14 FESEM images from the fracture surface area due to tensile test;A). Pure resin B). Nanocomposite containing 0.015% SGO

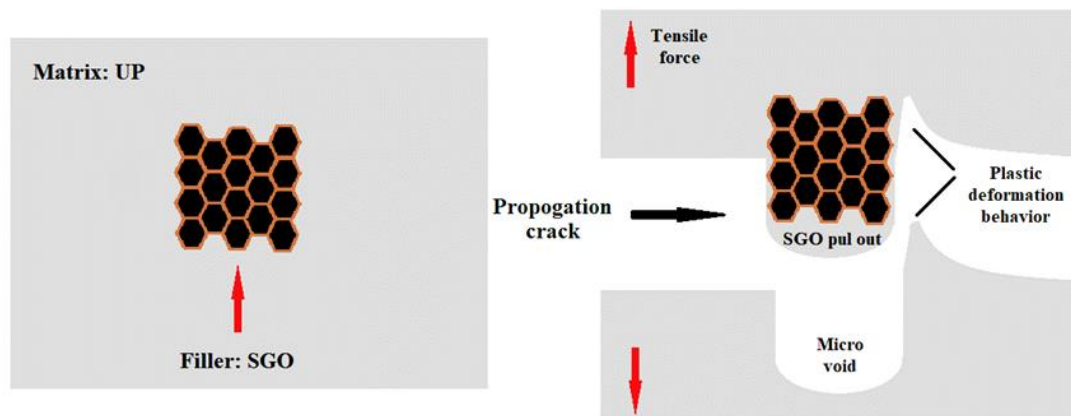


Fig. 15 Schematic of mechanism strengthening resin with SGO

Zeiss LEO 1455vp - Germany. Pure resin has a clean and smooth surface, which is a common characteristic of brittle resins (Fig. 13, part A). Adding SGO with a concentration of 0.015% showed that Nanosheets appeared on the fracture surface without aggregation (Fig. 13, part B). While increasing the concentration of SGO to 0.15%, more Nanosheets appeared on the fracture surface and accumulated in some places (Fig. 13, part C).

Mechanism discussion in illustration

The field emission scanning electron microscope (FESEM) model MIRA3-TESCAN-XMU was used to evaluate the surface morphology of NGORPs (zarei *et al.* 2018). The images (See Fig. 14) depict that the pure resin exhibits a notably low surface roughness. In contrast, adding 0.015% SGO resulted in an escalated surface roughness within the resin. This observation underscores the influential role of SGO in enhancing crack propagation resistance. The emergence of multi-level surface features

indicates crack deflection and the separation between the matrix and filler.

Based on the mechanisms stated in the past literature, in improving the polymer matrix's mechanical properties by GO, strengthening could be achieved by processes that perturb the cracks and dissipate their energy. This mechanism would allow for more significant elastic deformation, increased toughness, fracture strain, and strength (See Fig. 15) (Hussein *et al.* 2017).

The FESEM images from the fracture surface as a result of the tensile test are shown in Fig. 16; one of the main features of this surface morphology is the stepped surface structure indicated by arrows. It can be stated that the crack deflection mechanism, by tilting/twisting the crack, has led to the effective absorption of crack energy. When the crack path is disturbed by the Graphene Nanosheets, the crack tip is pinned and deflected near the sheet, then separates the sheets and propagates into the matrix.

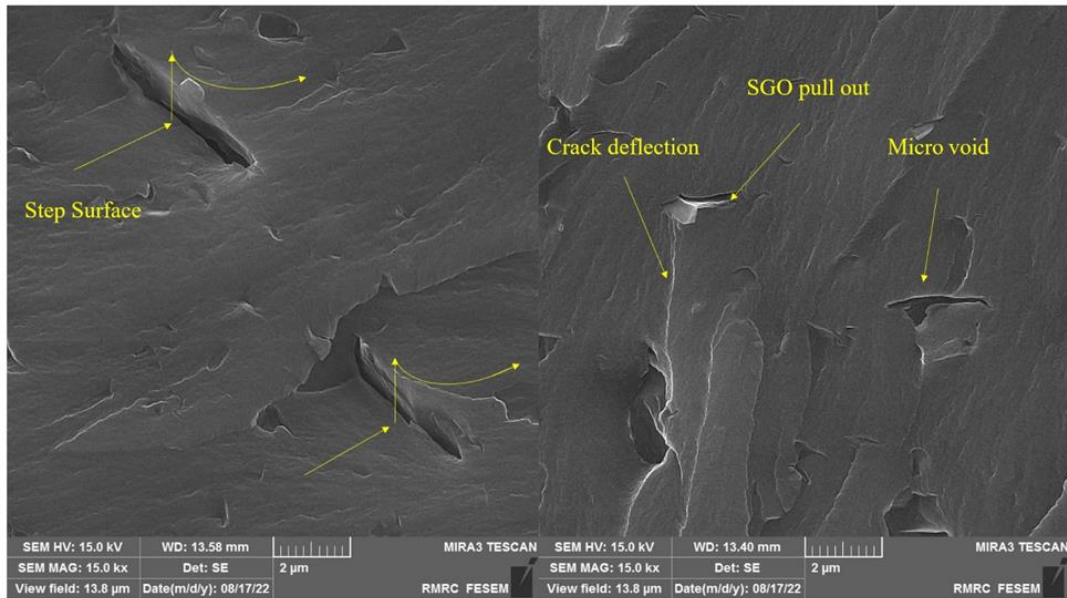


Fig. 16 FESEM images of the strengthening mechanism in nanocomposite containing 0.015% SGO

Table 3 Results of ASTM-D638 test on NGORP and base sample

Sample	Mechanical properties					
	Force(N)	Extension(mm)	Stress (MPa)	Elongation (%)	Energy(J)	TIME(Min)
Base	1869.74	0.8287	12.4793	1.6331	690.5156	0:10:06
GORP 0.015%	2615.35	2.4153	16.5979	4.017	2731.033	0:24:32
GORP 0.15%	574	22.3223	3.8300	41.9244	6267.1316	4:8:59

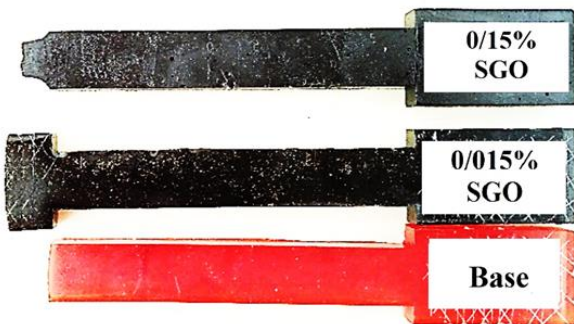


Fig. 17 The failure behavior in the base sample (purple) and the NGORP sample (black)

Mechanical properties

Adding 0.015% SGO during the NGORP manufacturing process enhanced all base sample properties. Additionally, NGORP-0.015% has the highest tolerance in applied force compared to NGORP-0.15% (Table 3). The tensile trial results showed that the applied energy for breaking a sample containing 0.015% SGO was 40% higher than for a base sample.

In Fig. 17, the ruptured place reveals that the SGO sample with a concentration of 0.015% is stronger than the base sample, as the fracture occurred near the clamp, not in the same area as the base sample. Therefore, the SGO sample was superior in strength to the base sample. Conversely, with an increased SGO concentration of 0.15%,

the sample exhibited diminished strength properties but notably increased flexibility. The higher flexibility of the NGORP-0.15% sample is evident from the observed necking phenomenon within the fracture area, as depicted in Fig. 17.

The comparison of plotted curves derived from tensile test data conducted on the fabricated samples in Fig. 18 provides a comprehensive evaluation of flexibility and brittle behavior. Observing the graph's linearity concerning the base resin and its in-situ rupture under applied tension, contrasted with the nanocomposites graph, reveals distinctive characteristics. The base sample appears inherently brittle, displaying no discernible flexibility.

In contrast, the composite manufactured with 0.15% Graphene oxide deviates from linear behavior, evading rupture even at maximum tensile strength, transitioning from the elastic to plastic deformation phase. The deformation of the plastic that appeared as a neck shape (as shown in Fig. 17) confirms its flexible nature. The nanocomposite containing 0.015% Graphene oxide exhibits properties between those of the base resin and the 0.15% Graphene oxide-nanocomposite. Its departure from linear behavior signifies an improvement in flexibility. Furthermore, its curve slope surpasses the 0.15% Graphene oxide nanocomposite, indicating heightened tolerance at the rupture point.

The results of this study are verified with previous studies in the literature that describe the fabrication of

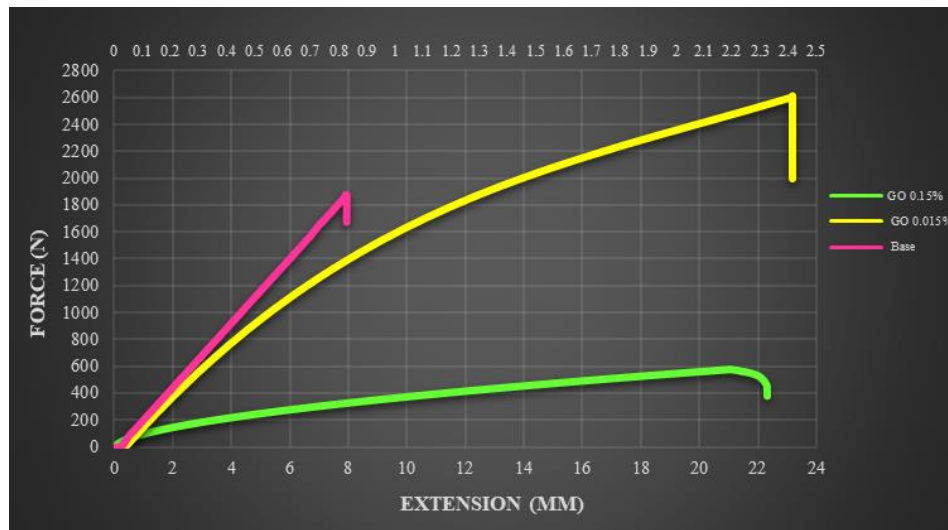


Fig. 18 Trial ASTM-D 638 results on all the constructed dog-bone samples

graphene oxide nanocomposites using unsaturated polyester resins. Bora *et al.* (2013) demonstrated that the addition of 3% Graphene oxide to unsaturated polyester resin led to a remarkable enhancement of 76% in tensile strength and a 41% increase in Young's (Bora *et al.* 2013) (Esmailzadeh *et al.* 2021). Furthermore, Swain (2013) reported that including Nano Graphene oxide at a concentration of 0.05% within unsaturated polyester resin resulted in a substantial 92% increase in bending strength compared to the pure resin (Swain, 2013).

Previous studies utilizing Graphene oxide Nanosheets in the fabrication of resins have encountered increased production costs due to high Nanosheet concentrations. Conversely, the approach introduced in this study involves the addition of a minute quantity, specifically 0.00015 gr, of single-layer Graphene oxide to unsaturated polyester resin. This method achieved a notable enhancement of 40% in strength properties and a substantial 120% improvement in elongation properties. This innovation aims to render the manufacturing process more cost-effective, providing a viable solution for affordable production.

4. Conclusions

In summary, this study demonstrates the significant impact of Single-Layer Graphene Oxide (SGO) Nanosheets on composite materials like unsaturated polyester resin, showcasing improved mechanical properties. Incorporating SGO Nanosheets fills nanoscale pores, thereby mitigating moisture ingress and the infiltration of detrimental ions, consequently inhibiting structural degradation.

The optimal concentration identified for fabricating Nanocomposites with Graphene Oxide Reinforced Polyester (NGORP) stands at 0.015%. This concentration exhibits enhancements across all strength parameters, notably achieving the highest increase in applied tensile force (745.61 N) and stress tolerance (4.1 MPa). Moreover, the NGORP manufactured at a 0.15% concentration showcases superior flexibility, which is evident in energy expenditure

for rupture (5576 j) and a 40% improvement in formability compared to the base sample. This exceptional flexibility qualifies it for producing parts requiring extraordinary flexibility properties.

A pivotal aspect of this study involves using low concentrations of Graphene Oxide Nanosheets, strategically considering economic factors. The extended lifespan of resin parts with minimal nanomaterial integration can substantially diminish maintenance costs. Thus, this research underlines a compelling rationale for employing nanomaterials on an industrial scale, enabling the fabrication of composite parts endowed with exceptional strength and elasticity.

References

- Bora, C., Gogoi, P., Baglari, S. and Dolui, S.K. (2013), "Preparation of polyester resin/graphene oxide nanocomposite with improved mechanical strength", *J. Appl. Polym. Sci.*, **129**(6), 3432-3438. <https://doi.org/10.1002/app.39068>
- Bouguerra, K., Ahmed, E.A., El-Gamal, S. and Benmokrane, B. (2011), "Testing of full-scale concrete bridge deck slabs reinforced with fiber-reinforced polymer (FRP) bars", *Constr. Build. Mater.*, **25**(10), 3956-3965. <https://doi.org/10.1016/j.conbuildmat.2011.04.028>
- Bousahla, A.A., Bourada, F., Mahmoud, S.R., Tounsi, A., Algarni, A., Bedia, E.A. and Tounsi, A. (2020), "Buckling and dynamic behavior of the simply supported CNT-RC beams using an integral-first shear deformation theory", *Comput. Concr.*, **25**(2), 155-166. <https://doi.org/10.12989/cac.2020.25.2.155>
- Chandradass, J., Ramesh Kumar, M. and Velmurugan, R. (2008), "Effect of clay dispersion on mechanical, thermal and vibration properties of glass fiber-reinforced vinyl ester composites", *J. Reinforc. Plast. Compos.*, **27**(15), 1585-1601. <https://doi.org/10.1177/0731684407081368>
- Davis, M.E. (2002), "Ordered porous materials for emerging applications", *Nature*, **417**(6891), 813-821. <https://doi.org/10.1038/nature00785>
- Esmailzadeh, M., Golmakani, M.E., Kadkhodayan, M., Amoozgar, M. and Bodaghi, M. (2021), "Geometrically nonlinear thermo-mechanical analysis of graphene-reinforced moving polymer nanoplates", *Adv. Nano Res.*, **10**(2), 151.

- <https://doi.org/10.12989/anr.2021.10.2.151>
- Farazin, A. and Mohammadimehr, M. (2020), "Nano research for investigating the effect of SWCNTs dimensions on the properties of the simulated nanocomposites: A molecular dynamics simulation", *Adv. Nano Res.*, **9**(2), 83-90. <https://doi.org/10.12989/anr.2020.9.2.083>
- Feng, Y., Zarei, V. and Mousavipour, N. (2023), "Provision and assessment properties of nanoliposomes containing macroalgae extracts of *Sargassum boveanum* and *Padina pavonica*", *LWT*, **175**, 114194. <https://doi.org/10.1016/j.lwt.2022.114194>
- Hammami, A. and Al-Ghuilani, N. (2004), "Durability and environmental degradation of glass-vinylester composites", *Polym. Compos.*, **25**(6), 609-616. <https://doi.org/10.1002/pc.20055>
- Huang, Z., Zhan, W. and Qian, X. (2020), "Challenges for lightweight composites in the offshore and marine industry from the fatigue perspective", *Compos. Mater. Eng.*, **2**(2), 65. <https://doi.org/10.12989/cme.2020.2.2.065>
- Hussein, A., Sarkar, S., Lee, K. and Kim, B. (2017), "Cryogenic fracture behavior of epoxy reinforced by a novel graphene oxide/poly (p-phenylenediamine) hybrid", *Compos. Part B Eng.*, **129**, 133-142. <https://doi.org/10.1016/j.compositesb.2017.07.085>
- Jang, B.Z. and Zhamu, A. (2008), "Processing of nanographene platelets (NGPs) and NGP nanocomposites: a review", *J. Mater. Sci.*, **43**(15), 5092-5101. <https://doi.org/10.1007/s10853-008-2755-2>
- Javani, R., Bidgoli, M.R. and Kolahchi, R. (2019), "Buckling analysis of plates reinforced by Graphene platelet based on Halpin-Tsai and Reddy theories", *Steel Compos. Struct.*, **31**(4), 419-426. <https://doi.org/10.12989/scs.2019.31.4.419>
- Johnson, D.W., Dobson, B.P. and Coleman, K.S. (2015), "A manufacturing perspective on graphene dispersions", *Curr. Op. Colloid Interf. Sci.*, **20**(5-6), 367-382. <https://doi.org/10.1016/j.cocis.2015.11.004>
- Khayat, M., Baghlani, A., Dehghan, S. M. and Najafgholipour, M. A. (2021), "The influence of graphene platelet with different dispersions on the vibrational behavior of nanocomposite truncated conical shells", *Steel Compos. Struct.*, **38**(1), 47-66. <https://doi.org/10.12989/scs.2021.38.1.047>
- Medani, M., Benahmed, A., Zidour, M., Heireche, H., Tounsi, A., Bousahla, A.A., Tounsi, A. and Mahmoud, S.R. (2019), "Static and dynamic behavior of (FG-CNT) reinforced porous sandwich plate using energy principle", *Steel Compos. Struct.*, **32**(5), 595-610. <https://doi.org/10.12989/scs.2019.32.5.595>
- Mirzaasadi, M., Zarei, V., Elveny, M., Alizadeh, S.M., Alizadeh, V. and Khan, A. (2021), "Improving the rheological properties and thermal stability of water-based drilling fluid using biogenic silica nanoparticles", *Energy Reports*, **7**, 6162-6171. <https://doi.org/10.1016/j.egy.2021.08.130>
- Park, H.K., Lee, S., Kim, Y.J., Jang, C. and Won, J. (2007), "Mechanical properties and microstructures of GFRP rebar after long-term exposure to chemical environments", *Polym. Polym. Compos.*, **15**(5), 403-408. <https://doi.org/10.1177/096739110701500508>
- Pokropivny, V.V. and Skorokhod, V.V. (2007), "Classification of nanostructures by dimensionality and concept of surface forms engineering in nanomaterial science", *Mater. Sci. Eng. C*, **27**(5-8), 990-993. <https://doi.org/10.1016/j.msec.2006.09.023>
- Shokrieh, M.M., Saeedi, A. and Chitsazzadeh, M. (2013), "Mechanical properties of multi-walled carbon nanotube/polyester nanocomposites", *J. Nanostruct. Chem.*, **3**(1), 1-5. <https://doi.org/10.1186/2193-8865-3-20>
- Signor, A.W., VanLandingham, M.R. and Chin, J.W. (2003), "Effects of ultraviolet radiation exposure on vinyl ester resins: characterization of chemical, physical and mechanical damage", *Polym. Degrad. Stabil.*, **79**(2), 359-368. [https://doi.org/10.1016/S0141-3910\(02\)00300-2](https://doi.org/10.1016/S0141-3910(02)00300-2)
- Swain, S. (2013), "Synthesis and characterization of graphene based unsaturated polyester resin composites", *Transact. Electr. Electr. Mater.*, **14**(2), 53-58. <https://doi.org/10.4313/TEEM.2013.14.2.53>
- Tounsi, A., Benguediab, S., Adda Bedia, E.A., Semmah, A. and Zidour, M. (2013), "Nonlocal effects on thermal buckling properties of double-walled carbon nanotubes", *Adv. Nano Res.*, **1**(1), 1. <https://doi.org/10.12989/anr.2013.1.1.001>
- Won, J.P., Lee, S.J., Jang, C.I. and Won, C. (2007), "Service life prediction of gfrp rebars in an alkaline environment", *Polym. Polym. Compos.*, **15**(6), 475-479. <https://doi.org/10.1177/096739110701500607>
- Won, J.P., Lee, S.J., Kim, Y.J., Jang, C.I. and Lee, S.W. (2008), "The effect of exposure to alkaline solution and water on the strength-porosity relationship of GFRP rebar", *Compos. Part B Eng.*, **39**(5), 764-772. <https://doi.org/10.1016/j.compositesb.2007.11.002>
- Zarei, V., Emamzadeh, A. and Nasiri, A. (2018), "Synthesis of amorphous silica nanoparticles from natural materials applied in drilling fluid for stabilizing shale layers", *J. Petrol. Res.*, **27**(96-6), 18-31.
- Zarei, V., Mirzaasadi, M., Davarpanah, A., Nasiri, A., Valizadeh, M. and Hosseini, M.J.S. (2021), "Environmental method for synthesizing amorphous silica oxide nanoparticles from a natural material", *Processes*, **9**(2), 334. <https://doi.org/10.3390/pr9020334>
- Zarei, V. and Nasiri, A. (2021), "Stabilizing Asmari Formation interlayer Shales using water-based mud containing biogenic silica oxide Nanoparticles synthesized", *J. Natural Gas Sci. Eng.*, 103928. <https://doi.org/10.1016/j.jngse.2021.103928>
- Zarei, V., Yavari, H., Nasiri, A., Mirzaasadi, M. and Davarpanah, A. (2023), "Implementation of amorphous mesoporous silica nanoparticles to formulate a novel water-based drilling fluid", *Arab. J. Chem.*, **16**, 104818. <https://doi.org/10.1016/j.arabjc.2023.104818>

AT